ISSN 0915-633X

NATIONAL INSTITUTE FOR FUSION SCIENCE

Anomalous Heat Evolution of Deuteron Implanted Al on Electron Bombardment

K. Kamada, H. Kinoshita and H. Takahashi

(Received - Apr. 15, 1994)

NIFS-281 May 1994

RESEARCH REPORT
NIFS Series

NAGOYA, JAPAN

Anomalous heat evolution of deuteron implanted Al on electron bombardment

K. Kamada, H. Kinoshita[1] and H. Takahashi[1]

National Institute for Fusion Science, Nagoya,

464-01 Japan.

[1]Department of Engineering, Hokkaido University,

Sapporo, 062 Japan

Abstract

Anomalous heat evolution was observed in deuteron implanted Al foils on 175 keV electron bombardment. Local regions with linear dimension of several 100nm showed simultaneous transformation from single crystalline to polycrystalline structure instantaneously on the electron bombardment, indicating the temperature rise up to more than melting point of Al from room temperature. The amount of energy evolved was more than 180MeV for each transformed region. The transformation was never observed in proton implanted Al foils. The heat evolution was considered due to a nuclear reaction in D_2 molecular collections.

Keywords: heat evolution, melting, aluminium, implantation, electron bombardment, transmission electron microscopy

1. Introduction

In a previous paper [1], one of the authors (K.K.) reported an anomalous particle emission phenomenon from H_3^+ or D_3^+ implanted Al foil

on 200 or 400keV electron bombardment. In the paper, the author presumed that fusion reactions to take place not only between deuterons but also between hydrogens, which were embedded in the so called "Tunnel Structure" (T.S.), created in sub-surface layers of Al on the implantations. (The results will be supplemented by more detailed experiments and also by theoretical considerations in a recent paper [2] .) One of the prominent features of this phenomenon was that it is not due to the energetic collisions between reacting particles. This was derived in the paper [1] from the calculation on the fusion reaction rate between knocked-on deuterons, produced by the electron bombardment, and embedded deuterons. In the present state of our knowledge, we cannot present any conclusive mechanism of the phenomenon, but the author presumes that β disintegration of proton on capturing of secondary electron in highly ionized hydrogen or deuteron plasma of nearly solid state density may play a fundamental role in the phenomenon, since the phenomenon is observable even in hydrogen implanted case.

In the present paper, a direct observation of this anomalous phenomenon via heat evolution leading to very local melting of deuterium implanted Al on 175 keV electron bombardment is reported. The direct observation was made by the transmission electron microscope (TEM), which at the same time served as an electron accelerator.

2. Experiment

We first implanted Al specimens with 25 keV D_2^+ ions. The specimens were prepared beforehand so as to enable TEM observations after the

implantation. They were polished chemically from Al disk with 5^{mm} diameter and 0.1^{mm} thick using TENUPOLE chemical polishing machine. The purity of the Al was 99.99%, and the specimens were annealed at 400℃ for 3 hours before the polishing. After the polishing they have wedge shape with average thickness of more than $1\,\mu$m over an area of about 1mm diameter and have a small hole of about 0.1mm diameter in the central part of each specimen.

The fluence of the implanted deuteron was chosen around 5×10^{17} D^{+}/cm^{2}, since below this amount of fluence only a bubble structure is formed in the sub-surface layer of Al foil, and above that so called "Tunnel Structure" (T.S.) is produced [3].

The density of the implanted deuterium in the T.S., 1×10^{22} $D_{2}cm^{-3}$, was also estimated from the same kind of experiment measuring the implanted amount of hydrogen during and after the implantation at room temperature [2,3]. Again from these experiments, the implanted deuterium are presumed to situate at about 100nm depth from the implanted surface. As a consequence, more than ten times of the implanted depth remains unimplanted beneath the T.S..

3. Experimental results

Two micrographs of Fig.1 show the typical examples of TEM observations taken on the Al specimens implanted with hydrogen, (a), and with deuteron, (b), respectively. Regions of brighter contrast in both micrographs are the T.S. regions, where Al atoms are lacked and, instead, hydrogen or deuterium molecules are contained. In the micrograph (b), we

can observe several areas, like the one indicated by an arrow, where something looks like microcrystallites are concentrated. These speckled areas appear instantaneously with the focusing of electron beam for the observation with a brighter contrast. They are not inherent to the implanted Al originally, but are attributable to the electron beam focusing effect. Before the focusing, when looking for the area to be observed with defocused beam, we can never observe such speckled areas. Further, these speckled areas can never be observable in hydrogen implanted Al under exactly the same experimental conditions with the deuteron implanted case. (So far we have done several ten times of the hydrogen implantation experiment.) This is readily seen in the micrograph (a) of Fig.1. To observe the speckled area, there is a region of optimum fluence of deuteron ions, which produce the microstructure like those shown in Fig.1. For lower fluence than that in the optimum region, we observe only bubble structures and never observe the speckled area, and for higher fluence, we observe, in addition to the T.S. structure, the bubble structure again but never observe the speckled area.

For crystallographic investigation of the speckled areas, selected area electron diffraction was tried on about 500nm area surrounding the speckled area. Those inserted in Fig.1 show the diffraction patterns taken on the areas seen in the micrographs. One should pay attention that (b-1) in Fig.1 (b), which was taken at the speckled area, clearly demonstrates the polycrystalline pattern with co-central spotty circular rings. On the other hand, the diffraction patterns from the normal areas, (a-1) and (b-2), show only usual Bragg spots showing single crystalline Al.

So far we have observed five polycrystalline rings from several speckled areas of different specimens. The lattice constants corresponding to the rings are tabulated in Table 1, together with the lattice constants and planes inhirent to Al.

To confirm the correspondence between the polycrystalline rings and the speckled area, dark field images were taken using several spots on the rings. Fig.2 (a) shows the bright field image of the speckled area with the diffraction rings, and (b) shows the dark field image of the same area taken with several diffraction spots on the rings. They show evidently that the polycrystalline spots originate from several parts of the speckled area, which appear brighter in (b).

The appearance of the speckled areas on the electron beam focusing is so rapid that we could not follow the detailed process of the appearance during the observation. However, after the appearance the images change rather gradually as seen in Fig.3. In this figure, (a) was taken in roughly 10 seconds or so after the appearance, and (b) and (c) were taken sequentially in less than 60 seconds after (a). These micrographs show rather gradual polycrystallization, judging from the growth of small crystallites as seen in (b) and (c), and the gradual change of equal thickness fringes as shown by an arrow. The change of the equal thickness fringes is presumed due to the thermal stress around the region. The image did not change anymore after (c).

These observations indicate a rapid melting and gradual crystallization, which is rather conceivable if we assume that the reactions in D_2 collections occurred suddenly and were maintained for a

short time, evolving the large amount of heat.

In addition to the above observations, we tried stereographic observations of the speckled region with change of the tilt angle of about 6 to 8 degrees to identify the depth of the layer in which the polycrystals are laying. As a result, we found that they are contained within the surface layer of the specimen with thickness of about 100nm above the T.S..

The experimental results described above clearly show that the speckled areas appeared on the electron bombardment is due to the local transformation from single crystalline to polycrystalline Al.

As far as the present authors are aware, the transformation from single crystalline to polycrystalline structure of Al metal with purity of 99.99% or above can never be achieved without melting and subsequent rapid solidification. One might inquire that the melting may induce evaporation of Al in high vacuum of electron microscope. However, the evaporation of Al on the melting does not take place usually due to the firm protection of the melt surface by the oxide film even after the chemical etching.

Now we evaluate the amount of the heat evolution necessary for the observed local melting. We know already that the implanted deuterium molecules aggregate at the depth of about 100nm from a surface on the implantation of 25 keV D_2^+, referring to the previous experiment with 25 keV H_2^+ [3] . From our observations so far undertaken, the extent of the transformed region occupies, on the average, $1 \times 10^{-9} cm^2$ of the surface. Taking the cover thickness of Al on the T.S. as 100nm, weight of Al

contained in the polycrystalline transformation becomes 2.7×10^{-14}g. The heat necessary to raise the temperature of this amount of Al from 300K to melting point 933K is $q = 633\times0.25\times2.7\times10^{-14} = 4.3\times10^{-12}$ cal, where the specific heat of Al in this temperature range is 0.25 cal/g · K. The latent heat of melting of Al is 2.58×10^{3} cal/mol [4], which gives the total latent heat for the melting of the above amount of Al $L = 2.58\times10^{3}\times2.7\times10^{-14}/27 = 2.58\times10^{-12}$ cal. Therefore, the whole heat necessary for the melting becomes, averaging on the several transformed regions, $Q = q + L = 6.9\times10^{-12}$ cal = 180 MeV for each transformed region.

Number of the deuterium molecules, which are the source of the heat evolution, contained in the T.S. just beneath the melted Al cover amounts to $1\times10^{-9}cm^{2}\times8\times10^{-6}cm\times1\times10^{22}cm^{-3} = 8\times10^{7}$ D_2 molecules, where the thickness of T.S. is 8×10^{-6}cm [3], density of the molecules in T.S. is $1\times10^{22}cm^{-3}$ and the area of the cover $1\times10^{-9}cm^{2}$ as before. So, if we assume that whole molecules just beneath the transformed area in the T.S. contribute to the melting, amount of the heat evolved per D_2 molecule becomes $180MeV/8\times10^{7}$ molecules = $2.3eV/D_2$.

Although this amount of the heat evolution per deuterium can be attributable to chemical reactions, we can not understand what kind of chemical reactions is responsible for the heat evolution, and why such chemical reactions take place only in deuterium in spite of the absence of the reaction in the chemically identical hydrogen collections. So we presume that the number of the molecules responsible for the melting may be far smaller than obtained above, and instead some kind of nuclear reactions occurred between the deuterium molecules, or between

deuterons, evolving such large amount of heat.

Here, we would like to mention that the above estimation of the energy evolution could be smaller than that of whole energy evolved, since we have totally neglected the heat conduction though Al specimen. As mentioned before, the bottom side of the specimen below the T.S. is far thicker than the top side. So, the large amount of heat evolved in the D_2 collections in T.S. is presumed to flow out of the specimen though the thick bottom part to the specimen holder. Therefore, the heat responsible for the melting of the top area of the specimen must be a part of the whole heat evolution.

4. Discussions

One of the authors (K.K.) has published a short paper [1] describing the particle emission from implanted Al on the electron bombardment. The present experimental results have close similarities with this particle emission experiment in two aspects. First of all, it is requisite to focus the electron beam to observe both the polycrystalline transformation and the particle emission. Secondly, the optimum implantation fluence around $\sim 5 \times 10^{17}$ ions/cm^2 is common in both experiments. Neither lower nor higher fluence does produce the heat evolution and the particle emission as well. We have to keep the fluence within roughly $\pm 10\%$ around the above value. However, the difference of the two kinds of experiment is that in the present experiment we could never observe the heat evolution in hydrogen implanted case, and, on the other hand, in the particle emission experiment, we could observe the particle emission in both hydrogen and

deuterium implanted cases. We presume that though the reactions in deuterium are accompanied with the heat evolution, the reactions in hydrogens, on the other hand, could be such as not accompaning the heat evolution. The two reactions are not necessarily the same reactions at all.

Here, we like to add that the primary electrons with energy around 200 keV has little interactions with the embedded deuterium, and hydrogen as well, in the present experimental conditions. However, internal secondary electrons produced in Al due to the primary electron bombardment have strong inelastic interactions with the deuterium leading to the nearly 100% ionization of them. In justification of this model, this interaction is capable of explaining the dependence of the phenomenon on both the electron beam focusing and the microstructure in the subsurface layer which are described above. These points will be discussed fully in [2] .

Reference

[1] K. Kamada ; Jpn. J. Appl. Phys. 31 L1289 (1992)

[2] preparing

[3] K. Kamada, A.Sagara, H. Kinoshita and H. Takahashi; Rad. Effects 103 119 (1987): K.Kamada; J. Nucl. Mater. 169 141 (1989).

[4] from American Institute of Physics Handbook, 3rd edition, McGraw Hill, New York, 1972.

Figure captions

Fig.1 Transmission electron micrographs of hydrogen, (a), and deuterium, (b), implanted Al. An example of the polycrystallized area on the electron bombardment is shown by an arrow in (b). Selected area diffraction patterns taken on normal T.S. area, (a-1) and (b-2), and that taken on the polycrystallized area, (b-1), are inserted.

Fig.2 Bright field, (a), and dark field, (b), images taken on the polycrystallized area in a deuterium implanted Al. The dark field image was taken with several diffraction spots on the circular rings of the inserted selcted area diffraction pattern.

Fig.3 Sequential TEM micrographs of the same area of a derterium implanted Al, which were taken in less than 60 seconds after the appearance of the speckled area. (a) was taken in less than 10 second, then (b) and (c) were taken in less than 60 seconds sequentially after (a).

Table 1 Lattice constants of the polycrystalline aggregates determined by electron diffraction with the camera length L=570mm and the wavelength of electron λ=2.99×10-3nm. Lattice constants and corresponding lattice planes of Al are shown together for reference purpose.

Ring	d_{obs}(A)	d_{obs}(A)	d_{obs}(A)	d_{obs}(A)	d_{obs}(A)(hkl)
1	2.4024	2.3976	2.3549	2.3385	2.338(111)
2	2.0366	2.0609	2.0287	-	2.024(200)
3	1.4570	1.4511	1.4505	-	1.431(220)
4	1.2473	1.2398	1.2213	-	1.221(311)
5	0.9266	-	-	-	0.9289(331)

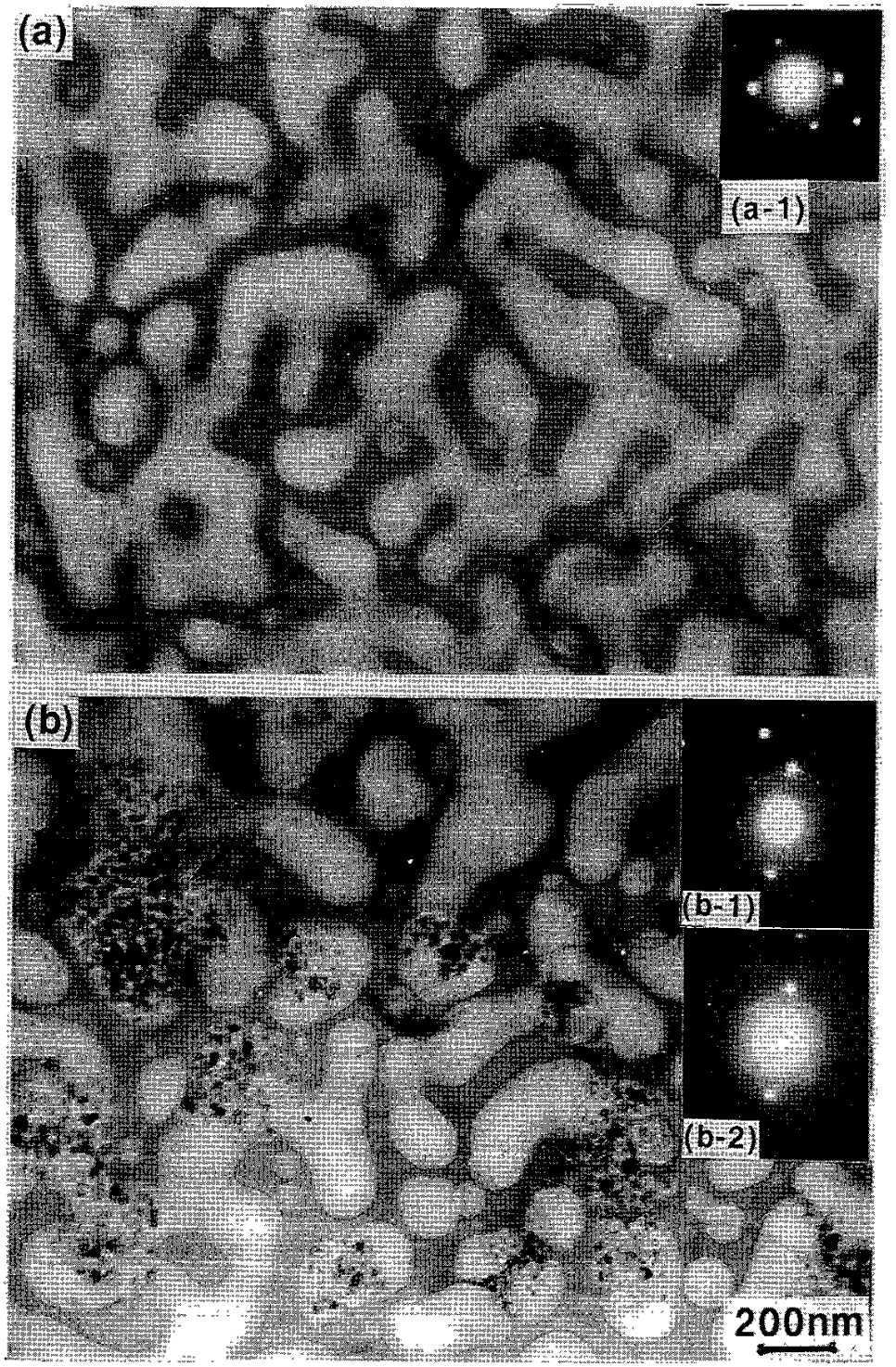

Fig.1

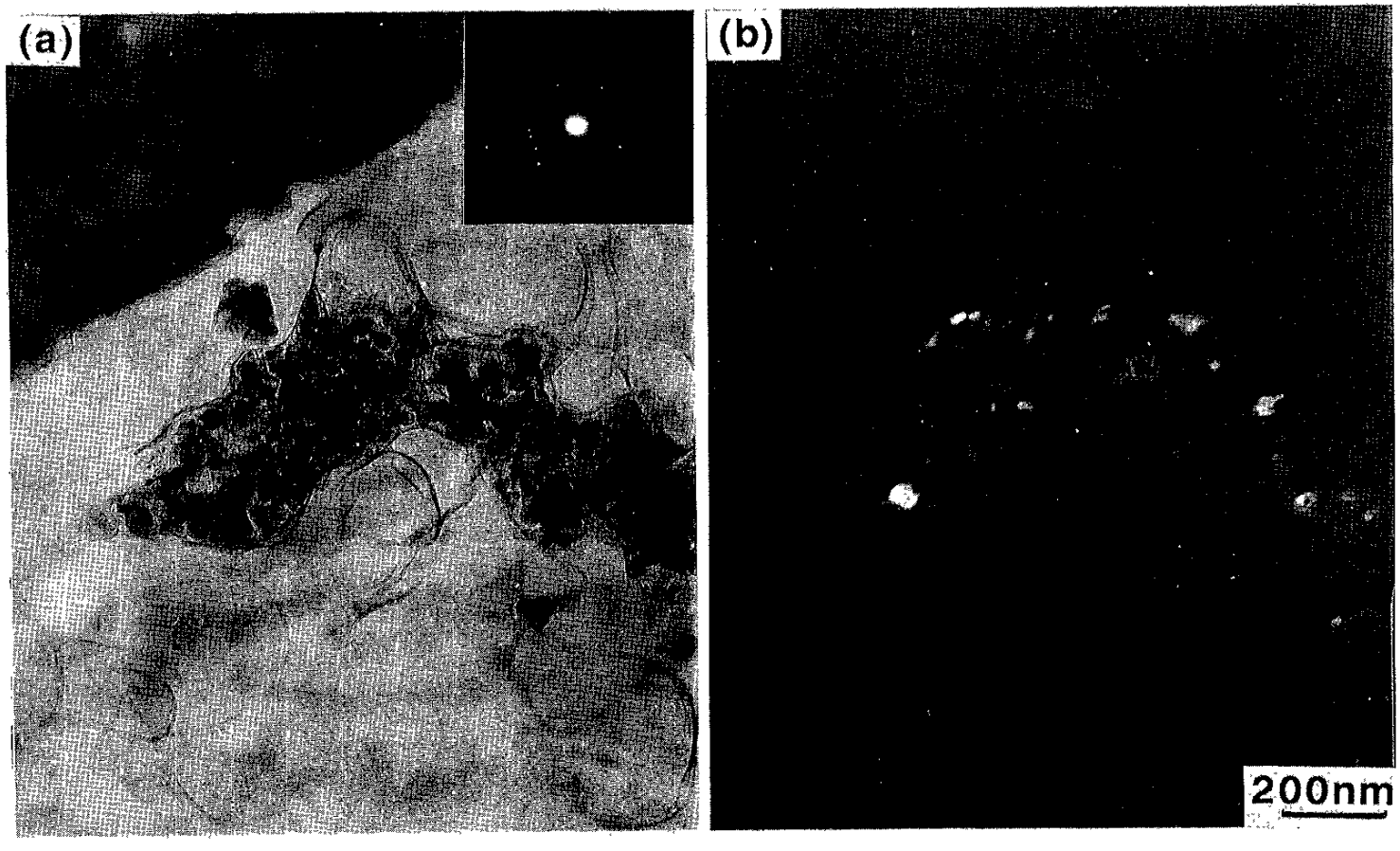

Fig. 2

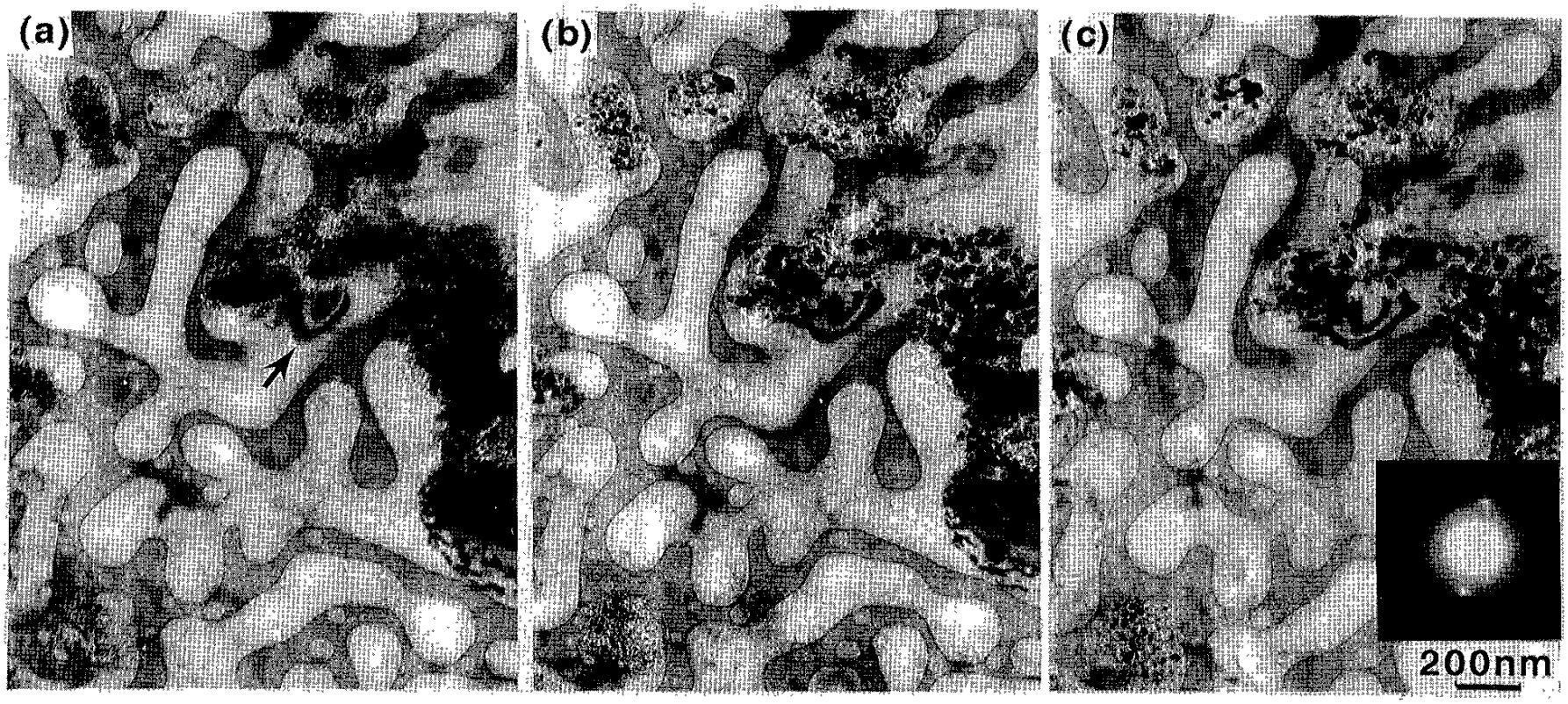

Fig. 3

Recent Issues of NIFS Series

NIFS-236 A. Fujisawa and Y. Hamada, *Theoretical Study of Cylindrical Energy Analyzers for MeV Range Heavy Ion Beam Probes;* July 1993

NIFS-237 N. Ohyabu, A. Sagara, T. Ono, T. Kawamura and O. Motojima, *Carbon Sheet Pumping;* July 1993

NIFS-238 K. Watanabe, T. Sato and Y. Nakayama, *Q-profile Flattening due to Nonlinear Development of Resistive Kink Mode and Ensuing Fast Crash in Sawtooth Oscillations;* July 1993

NIFS-239 N. Ohyabu, T. Watanabe, Hantao Ji, H. Akao, T. Ono, T. Kawamura, K. Yamazaki, K. Akaishi, N. Inoue, A. Komori, Y. Kubota, N. Noda, A. Sagara, H. Suzuki, O. Motojima, M. Fujiwara, A. Iiyoshi, *LHD Helical Divertor;* July 1993

NIFS-240 Y. Miura, F. Okano, N. Suzuki, M. Mori, K. Hoshino, H. Maeda, T. Takizuka, JFT-2M Group, K. Itoh and S.-I. Itoh, *Ion Heat Pulse after Sawtooth Crash in the JFT-2M Tokamak;* Aug. 1993

NIFS-241 K. Ida, Y.Miura, T. Matsuda, K. Itoh and JFT-2M Group, *Observation of non Diffusive Term of Toroidal Momentum Transport in the JFT-2M Tokamak;* Aug. 1993

NIFS-242 O.J.W.F. Kardaun, S.-I. Itoh, K. Itoh and J.W.P.F. Kardaun, *Discriminant Analysis to Predict the Occurrence of ELMS in H-Mode Discharges;* Aug. 1993

NIFS-243 K. Itoh, S.-I. Itoh, A. Fukuyama, *Modelling of Transport Phenomena;* Sep. 1993

NIFS-244 J. Todoroki, *Averaged Resistive MHD Equations;* Sep. 1993

NIFS-245 M. Tanaka, *The Origin of Collisionless Dissipation in Magnetic Reconnection;* Sep. 1993

NIFS-246 M. Yagi, K. Itoh, S.-I. Itoh, A. Fukuyama and M. Azumi, *Current Diffusive Ballooning Mode in Seecond Stability Region of Tokamaks;* Sep. 1993

NIFS-247 T. Yamagishi, *Trapped Electron Instabilities due to Electron Temperature Gradient and Anomalous Transport;* Oct. 1993

NIFS-248 Y. Kondoh,

Attractors of Dissipative Structure in Three Disspative Fluids; Oct. 1993

NIFS-249 S. Murakami, M. Okamoto, N. Nakajima, M. Ohnishi, H. Okada, *Monte Carlo Simulation Study of the ICRF Minority Heating in the Large Helical Device;* Oct. 1993

NIFS-250 A. Iiyoshi, H. Momota, O. Motojima, M. Okamoto, S. Sudo, Y. Tomita, S. Yamaguchi, M. Ohnishi, M. Onozuka, C. Uenosono, *Innovative Energy Production in Fusion Reactors*; Oct. 1993

NIFS-251 H. Momota, O. Motojima, M. Okamoto, S. Sudo, Y. Tomita, S. Yamaguchi, A. Iiyoshi, M. Onozuka, M. Ohnishi, C. Uenosono, *Characteristics of D-^{3}He Fueled FRC Reactor: ARTEMIS-L,* Nov. 1993

NIFS-252 Y. Tomita, L.Y. Shu, H. Momota, *Direct Energy Conversion System for D-^{3}He Fusion,* Nov. 1993

NIFS-253 S. Sudo, Y. Tomita, S. Yamaguchi, A. Iiyoshi, H. Momota, O. Motojima, M. Okamoto, M. Ohnishi, M. Onozuka, C. Uenosono, *Hydrogen Production in Fusion Reactors,* Nov. 1993

NIFS-254 S. Yamaguchi, A. Iiyoshi, O. Motojima, M. Okamoto, S. Sudo, M. Ohnishi, M. Onozuka, C. Uenosono, *Direct Energy Conversion of Radiation Energy in Fusion Reactor,* Nov. 1993

NIFS-255 S. Sudo, M. Kanno, H. Kaneko, S. Saka, T. Shirai, T. Baba, *Proposed High Speed Pellet Injection System "HIPEL" for Large Helical Device* Nov. 1993

NIFS-256 S. Yamada, H. Chikaraishi, S. Tanahashi, T. Mito, K. Takahata, N. Yanagi, M. Sakamoto, A. Nishimura, O. Motojima, J. Yamamoto, Y. Yonenaga, R. Watanabe, *Improvement of a High Current DC Power Supply System for Testing the Large Scaled Superconducting Cables and Magnets*; Nov. 1993

NIFS-257 S. Sasaki, Y. Uesugi, S. Takamura, H. Sanuki, K. Kadota, *Temporal Behavior of the Electron Density Profile During Limiter Biasing in the HYBTOK-II Tokamak*; Nov. 1993

NIFS-258 K. Yamazaki, H. Kaneko, S. Yamaguchi, K.Y. Watanabe, Y.Taniguchi, O.Motojima, LHD Group, *Design of Central Control System for Large Helical Device (LHD)*; Nov. 1993

NIFS-259 S. Yamada, T. Mito, A. Nishimura, K. Takahata, S. Satoh, J. Yamamoto,

H. Yamamura, K. Masuda, S. Kashihara, K. Fukusada, E. Tada,
Reduction of Hydrocarbon Impurities in 200L/H Helium Liquefier-Refrigerator System; Nov. 1993

NIFS-260 B.V.Kuteev,
Pellet Ablation in Large Helical Device; Nov. 1993

NIFS-261 K. Yamazaki,
Proposal of "MODULAR HELIOTRON': Advanced Modular Helical System Compatible with Closed Helical Divertor; Nov. 1993

NIFS-262 V.D.Pustovitov,
Some Theoretical Problems of Magnetic Diagnostics in Tokamaks and Stellarators; Dec. 1993

NIFS-263 A. Fujisawa, H. Iguchi, Y. Hamada
A Study of Non-Ideal Focus Properties of 30° Parallel Plate Energy Analyzers; Dec. 1993

NIFS-264 K. Masai,
Nonequilibria in Thermal Emission from Supernova Remnants; Dec. 1993

NIFS-265 K. Masai, K. Nomoto,
X-Ray Enhancement of SN 1987A Due to Interaction with its Ring-like Nebula; Dec. 1993

NIFS-266 J. Uramoto
A Research of Possibility for Negative Muon Production by a Low Energy Electron Beam Accompanying Ion Beam; Dec. 1993

NIFS-267 H. Iguchi, K. Ida, H. Yamada, K. Itoh, S.-I. Itoh, K. Matsuoka, S. Okamura, H. Sanuki, I. Yamada, H. Takenaga, K. Uchino, K. Muraoka,
The Effect of Magnetic Field Configuration on Particle Pinch Velocity in Compact Helical System (CHS); Jan. 1994

NIFS-268 T. Shikama, C. Namba, M. Kosuda, Y. Maeda,
Development of High Time-Resolution Laser Flash Equipment for Thermal Diffusivity Measurements Usting Miniature-Size Specimens; Jan. 1994

NIFS-269 T. Hayashi, T. Sato, P. Merkel, J. Nührenberg, U. Schwenn,
Formation and 'Self-Healing' of Magnetic Islands in Finite-β Helias Equilibria; Jan. 1994

NIFS-270 S. Murakami, M. Okamoto, N. Nakajima, T. Mutoh,
Efficiencies of the ICRF Minority Heating in the CHS and LHD Plasmas; Jan. 1994

NIFS-271 Y. Nejoh, H. Sanuki,
Large Amplitude Langmuir and Ion-Acoustic Waves in a Relativistic Two-Fluid Plasma; Feb. 1994

NIFS-272 A. Fujisawa, H. Iguchi, A. Taniike, M. Sasao, Y. Hamada,
A 6MeV Heavy Ion Beam Probe for the Large Helical Device;
Feb. 1994

NIFS-273 Y. Hamada, A. Nishizawa, Y. Kawasumi, K. Narihara, K. Sato, T. Seki, K. Toi, H. Iguchi, A. Fujisawa, K. Adachi, A. Ejiri, S. Hidekuma, S. Hirokura, K. Ida, J. Koong, K. Kawahata, M. Kojima, R. Kumazawa, H. Kuramoto, R. Liang, H. Sakakita, M. Sasao, K. N. Sato, T. Tsuzuki, J. Xu, I. Yamada, T. Watari, I. Negi,
Measurement of Profiles of the Space Potential in JIPP T-IIU Tokamak Plasmas by Slow Poloidal and Fast Toroidal Sweeps of a Heavy Ion Beam; Feb. 1994

NIFS-274 M. Tanaka,
A Mechanism of Collisionless Magnetic Reconnection; Mar. 1994

NIFS-275 A. Fukuyama, K. Itoh, S.-I. Itoh, M. Yagi and M. Azumi,
Isotope Effect on Confinement in DT Plasmas; Mar. 1994

NIFS-276 R.V. Reddy, K. Watanabe, T. Sato and T.H. Watanabe,
Impulsive Alfven Coupling between the Magnetosphere and Ionosphere, Apr.1994

NIFS-277 J. Uramoto,
A Possibility of π^- Meson Production by a Low Energy Electron Bunch and Positive Ion Bunch, Apr. 1994

NIFS-278 K. Itoh, S.-I. Itoh, A. Fukuyama, M. Yagi and M. Azumi,
Self-sustained Turbulence and L-mode Confinement in Toroidal Plasmas II, Apr. 1994

NIFS-279 K. Yamazaki and K.Y.Watanabe,
New Modular Heliotron System Compatible with Closed Helical Divertor and Good Plasma Confinement, Apr. 1994

NIFS-280 S. Okamura, K. Matsuoka, K. Nishimura, K. Tsumori, R. Akiyama, S. Sakakibara, H. Yamada, S. Morita, T. Morisaki,. N. Nakajima, K. Tanaka, J. Xu, K. Ida, H. Iguchi, A. Lazaros, T. Ozaki, H. Arimoto, A. Ejiri, M. Fujiwara, H. Idei. O. Kaneko, K. Kawahata, T. Kawamoto, A. Komori, S. Kubo, O. Motojima, V.D. Pustovitov, C. Takahashi, K. Toi and I. Yamada,
High-Beta Discharges with Neutral Beam Injection in CHS,
Apr. 1994